Bioorganic Chemistry 82 (2019) 192–203

Contents lists available at ScienceDirect

Bioorganic Chemistry

journal homepage: www.elsevier.com/locate/bioorg

Hydrogen sulfide releasing enmein-type diterpenoid derivatives as apoptosis inducers through mitochondria-related pathways

Fanxing Xu[a,b], Xiang Gao[a], Haonan Li[a], Shengtao Xu[c], Xu Li[d], Xu Hu[a], Zhanlin Li[a], Jinyi Xu[c], Huiming Hua[a], Dahong Li[a,*]

[a] Key Laboratory of Structure-Based Drug Design & Discovery, Ministry of Education, and School of Traditional Chinese Materia Medica, Shenyang Pharmaceutical University, 103 Wenhua Road, Shenyang 110016, PR China
[b] Wuya College of Innovation, Shenyang Pharmaceutical University, 103 Wenhua Road, Shenyang 110016, PR China
[c] Department of Medicinal Chemistry and State Key Laboratory of Natural Medicines, China Pharmaceutical University, 24 Tongjia Xiang, Nanjing 210009, PR China
[d] Jiangsu Kanion Pharmaceutical Co., Ltd., 58 Kangyuan Road, Lianyungang 222001, PR China

ARTICLE INFO

Keywords:
Enmein-type diterpenoid
Hydrogen sulfide
Apoptosis
Mitochondria-related pathway

ABSTRACT

In this study, we combined two enemin-type diterpenoid derivatives with two well-established hydrogen sulfide moieties via ester or different anhydride linkers, to search apoptosis inducing drug candidate capable of hydrogen sulfide generating. Therefore, a series of hybrids were synthesized and superior antiproliferative efficacy accompanied with enhanced selectivity was observed under extensive pharmacological evaluations. A standard methylene blue (MB^+) method was applied to measure the capacity for the hydrogen sulfide generation of all the target derivatives. One particular molecule **A1**, which contained *α*-thioctic acid moiety for hydrogen sulfide donating, manifested more potent antiproliferative activity. It exerted inhibitory effects against Bel-7402, SGC-7901 and A549 cell lines with IC_{50} values of 2.16, 5.07 and 6.98 μM respectively. While it exacted relatively low effects over human normal cell lines L-02 and PBMC with IC_{50} values of 15.81 μM for the prior and 14.15 μM for the latter, and displayed better selectivity index (SI) than parent diterpenoids. A high dosage of H_2S release was also recorded. Hence, **A1** was most suitable for mechanistic exploration on account of both safety and efficacy. The ensuing biological assays revealed central role of apoptosis in **A1**'s mode of action for antiproliferative efficacy, which led to further confirmation of G1 phase cell cycle arrest, mitochondria membrane potential collapse and apoptotic activation in Bel-7402 cells. Further western blot assay on intrinsic mitochondria pathway unlocked intricate interplay among a series of apoptotic related proteins in which Bax, caspase-3 and cytochrome *c* went through up-regulation, while Bcl-2, Bcl-xL and procaspase-3 undergone down-regulation. In a nutshell, a hydrogen sulfide releasing hybrid **A1** was synthesized and antiproliferative evaluation identified it to be a worthy drug candidate for future in depth study.

1. Introduction

Total 51% new approved drugs originated from or partially comprised of natural products between 1981 and 2014, which affirmed the position of natural resource as a focal point in finding structural and medicinal inspiration for drug discovery [1]. As a genus known for its complex ring system and numerous biological properties, diterpenoids offered a string of approved drugs like andrographolide [2–6], ginkgolides [7–10] and paclitaxel [11–13] to clinical application, in the meantime would have more potential lead compounds or modified derivatives forthcoming. One particular sub-type, 6,7-*seco*-*ent*-kaurane diterpenoids, owned its speedy research to the unique scaffolds and distinct biological effects of oridonin or enmein [14–20]. After first discovery from *Isodon* species in 1976, which belonged to a common yet valuable genus of the Labiatae family, oridonin was uncovered with potent anticancer efficacy and displayed notable cytotoxicity against leukemia [21], human lung cancer [22], gastric cancer [23], pancreatic cancer [24], colon tumor [25], liver cancer [26] and esophageal cancer [27]. Despite isolated in a much early date of 1958, from the same plant of *Isodon*, however, the same amount of attention failed to fall on enmein-type diterpenoids, which too, possessed potent antiproliferative activities against a broad range of tumorous malignancy including liver cancer [28], lung cancer [28], bladder cancer [29], leukemia [15], cervical cancer [30] plus prostate cancer [31] and provided an intriguing skeleton rich in stereogenic positions. The main cause of this impediment, besides relatively moderate effect and insufficient

* Corresponding author.
E-mail address: lidahong0203@163.com (D. Li).

https://doi.org/10.1016/j.bioorg.2018.10.002
Received 14 June 2018; Received in revised form 21 September 2018; Accepted 4 October 2018
Available online 08 October 2018
0045-2068/

selectivity [32], was the confinement of accessibility to naturally occurred enmein-type structures. Hence, only after an efficient route of conversion from natural oridonin to enmein-type molecules established [20], did modificational exploration gained momentum [33–38]. In depth studies on antitumor effects and mechanistic patterns of enmein-type derivatives revealed that cell cycle arrest, mitochondria pathway anomaly and a series of apoptotic proteins all interacted closely in inducing apoptosis and in turn brought about cytotoxic effects [39]. More efforts on biological evaluation remain in urgent need. This comparably unexploited status manifested that endeavors still warranted to further diversify enmein-type structural library and to complement the study to mode of action underpinning various pharmacological efficacy in search of potential anticancer therapeutics.

The first discovery of nitric oxide as signaling gastransmitter, which mediated in multifarious physiological and pathological conditions, transformed the landscape for medicinal study. Since 1990s, two more significant gaseous molecules, carbon monoxide and hydrogen sulfide (H_2S), were rediscovered their roles as key mediators for both *in vitro* and *in vivo* bio-activities [40]. Among them, H_2S was under intensive research for its therapeutic properties stretching extensively from well-studied cardiovascular problems such as hypertension [41], stroke [42], ischemia-reperfusion injury [43] to atherosclerosis [44], diabetic diseases [45] and neuroinflammation [46]. Additionally, the occurrence of endogenous H_2S was well-understood, which involved three cellar conversion of lead enzymes: cystathionine-γ-lyase (CSE), cystathionine-β-synthase (CBS) and 3-mercaptopyruvate sulfurtransferase (MST) with corresponding substrates: L-cysteine and homocysteine for both CSE and CBS, while 3-mercaptopyruvate was converted by MST [47,48]. One particular effect, tumor related function, trapped our attention through perplexing yet intriguing side switching between cytoprotective and cytotoxic efficacy to tumor cells and interesting mechanistic pathways including EGFR/ERK/MMP-2 [49], PI3K/Akt/mTOR [50] and p38/MAPK [51,52] against various cancer cells. Recent studies elucidated the pinpoint existed in H_2S induced antitumor activities, in which a watershed dosage of gaso-donor manipulated the H_2S generated endogenously either to spur proliferation of malignancy [53–56] or opt for exerting substantial cytotoxicity towards cancerous cells [57]. The prior results stemmed from the relative high expression of CBS in prostate [53], colon [54], breast [55], ovarian [56] and other tumor cells. Targeted inhibition of CBS resulted in sufficiently suppressed tumor growth, principally associated with cell cycle disturbance, mitochondria dysfunction and brought on the activation of apoptotic proteins, and finally apoptosis [58–60]. However, the lack of H_2S derivatives had long been pestering researchers, and was tackle by subsequent works in which various good H_2S donating compounds were developed (like α-thioctic acid, ADTOH, thiobenzamide, tetrasulfides, cyclic acyl disulfides, acyl selenylsulfides and iminothioethers, Fig. 1) [61–71]. Additionally, recent research demonstrated that compounds incorporated with thioctic acid which retained hypoglycaemic ability didn't cause low blood sugar in normal circumstances [72]. Presented

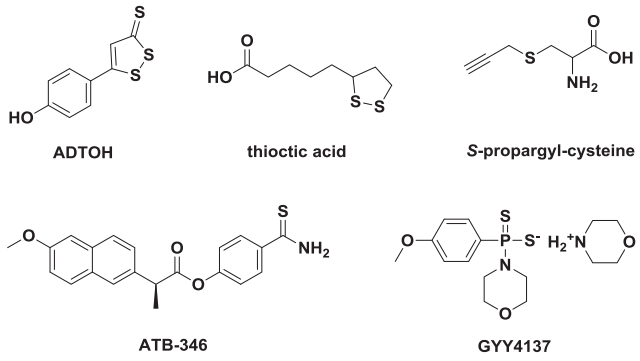

Fig. 1. Chemical structures of selected H_2S donating derivatives.

with this opportunity, we decided to tap into this reserve of H_2S releasing moieties with synthetic method of combination principle to construct novel hybrids with desirable antiproliferative efficacy.

Hence, we strove to harness the extensive anticancer activities of both molecules through synergetic boost of efficacy by utilizing joint advantages. In this study, two enmein-type cores (**2** and **3**) were conjugated with two stable hydrogen sulfide generating moieties (ADTOH and thioctic acid), bridged via ester or anhydride linkers. The antiproliferative evaluation was carried out against three tumor cell lines: liver cancer Bel-7402, gastric cancer SGC-7901, lung cancer A549 cell line while two normal cell lines were tested: human normal liver L-02 and human normal peripheral blood mononuclear cell line (PBMC). Further experiments into mechanisms behind inhibitory effects of lead compound **A1** were also performed, including cell cycle progression, apoptotic induction, mitochondria membrane potential disruption and the expression of apoptotic proteins.

2. Result and discussion

2.1. Chemistry

The overall synthetic route was outlined in Scheme 1. Starting with anethole trithione, pyridine hydrochloride was added, and the solid was melted under apron protection, then cooling to 100 °C to mix water for filtration. The resulting mixture was first basified by 10% sodium hydroxide then acidified by concentrated hydrochloric acid to afford crude product in red color. ADTOH was finally attained through neutralizing the crude product by water. The enmein-type diterpenoid core **2** was converted from commercially acquired oridonin **1** which was oxidated by sodium periodate in water for over 90% yield. Further treatment of Jones reagent selectively oxidized the 6-OH of **2** gave ketone **3**. Both reactions were achieved with good yields above 90%. Hybrid, **A1**, was afforded through direct reaction of **2** with α-thioctic acid under the condition of 4-dimethylaminopyridine (DMAP) and 1-ethyl-3-(3-dimethylaminopropyl) carbodiimide hydrochloride (EDCI) in DCM at room temperature. Intermediates **6–12** were obtained through esterification between diterpenoid derivatives and corresponding anhydride under the condition of DMAP and triethylamine (TEA) in dichloromethane (DCM) at room temperature. Then, hybrids **B1–4** and **C1–3** were acquired through condensation of corresponding intermediate with H_2S donor ADTOH in DCM in the presence of DMAP and dicyclohexylcarbodiimide (DCC) at −5 °C.

2.2. Biological evaluation

2.2.1. Cytotoxic activity and structure-activity relationships analysis

The antiproliferative activities of target hybrids (**A1**, **B1–4** and **C1–3**), parental diterpenoids (**1** and **2**) and H_2S donors (ADTOH and α-thioctic acid) were evaluated by a standard 3-(4,5-dimethylthiazol-2-yl)-2,5-diphenyltetrazolium bromide (MTT) experiment. A set of four different cell lines (Bel-7402, SGC-7901, A549 and L-02) were selected for aforementioned test. And 5-FU was chosen as positive control. All test results were summarized in Table 1.

A straight answer could be draw from the inhibitory results of two H_2S donors ADTOH and α-thioctic acid and target conjugates **B1–4**. No significant effects were observed on both tumor and normal cell lines according to cytotoxic data (with IC_{50} values over 50 μM), except for **B1** with low cytotoxicity against Bel-7402 and SGC-7901 tumor cells (IC_{50} values were 40.39 and 41.64 μM, respectively). Went through it separately, however, we reasoned that ineffectual antiproliferative activities of ADTOH and α-thioctic acid above 50 μM were in fact a manifestation of relatively high dosage required to achieve inhibition, which stood at millimolar level according to literature [73]. On the other hand, the hybrids, which comprised of enmein-type core **2** substituted by two ADTOH moieties through both 6-/14-OH anhydride linkers (**B2**, **B3** and **B4**), exhibited same poor results as H_2S donors. Hence, additional

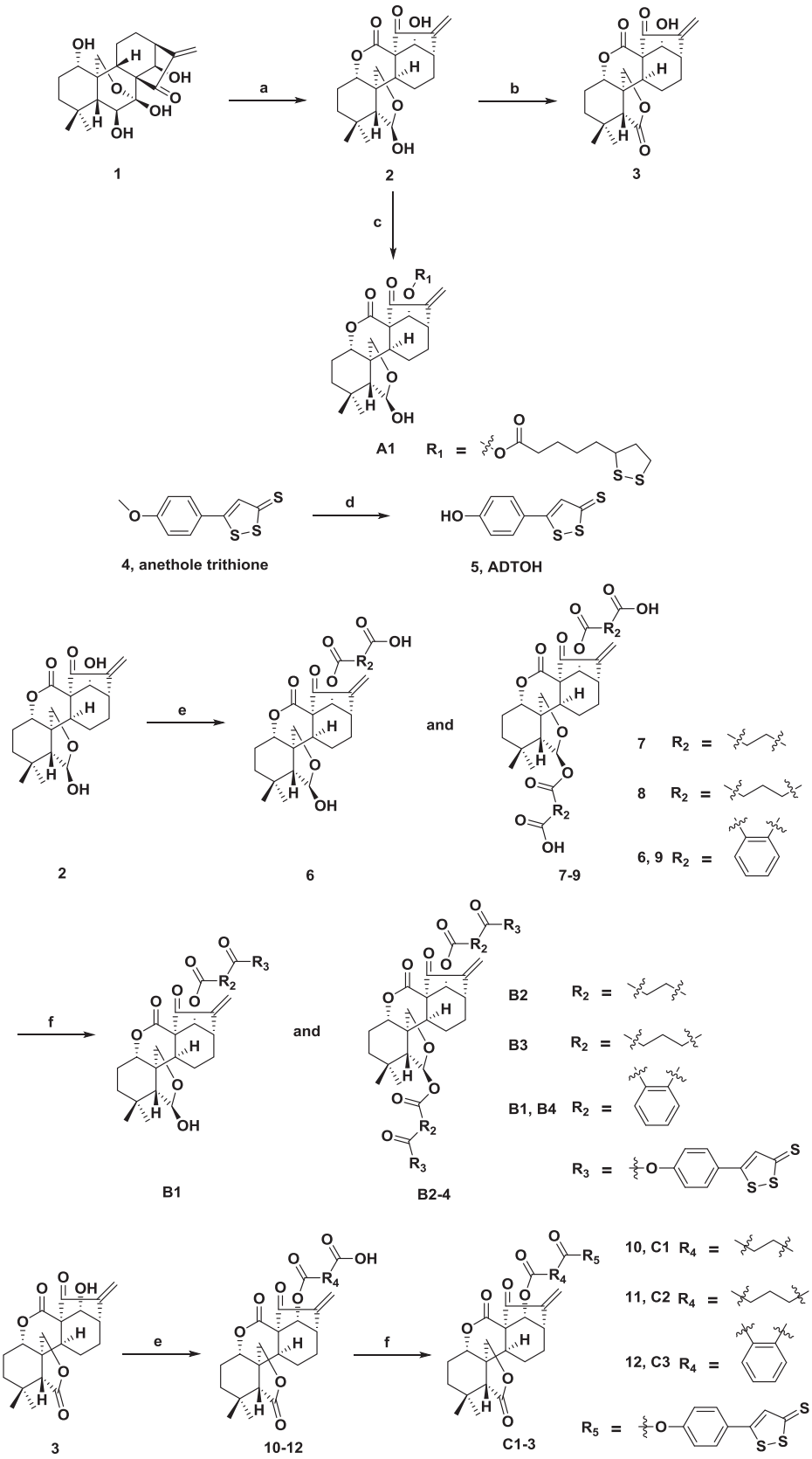

Scheme 1. Synthesis of derivatives **A1**, **B1–4** and **C1–3**. *Reagents and conditions*: (a) sodium periodate, H_2O, rt, 6 h; (b) Jones reagent, DCM, rt, 0.5 h; (c) EDCI, DMAP, DCM, rt, 12 h; (d) pyridine hydrochloride, argon, 215 °C, 20 min; (e) correspondent anhydride, EDCI, DMAP, DCM, rt, 8–12 h; (f) ADTOH, DCC, DMAP, DCM, −5 °C, 6–16 h.

Table 1
Antiproliferative activities of enmein derivatives and hydrogen sulfide donors against three cancerous and two normal cell lines.

Compound	IC_{50} (μM)[a]					
	Bel-7402	SGC-7901	A-549	L-02	PBMC	SI[b]
Oridonin (1)	7.85 ± 0.37	7.13 ± 0.29	18.15 ± 1.28	19.53 ± 1.10	NT[c]	2.5
2	23.18 ± 1.63	28.54 ± 1.28	27.56 ± 2.94	25.47 ± 1.34	NT	1.1
ADTOH	> 50	> 50	> 50	> 50	NT	NC[d]
Thioctic acid	> 50	> 50	> 50	> 50	NT	NC
A1	2.16 ± 0.24	5.07 ± 0.20	6.98 ± 0.15	15.81 ± 0.52	14.15 ± 0.60	7.3
B1	40.39 ± 1.93	41.64 ± 2.48	> 50	> 50	NT	> 1.2
B2	> 50	> 50	> 50	> 50	NT	NC
B3	> 50	> 50	> 50	> 50	NT	NC
B4	> 50	> 50	> 50	> 50	NT	NC
C1	20.48 ± 1.52	20.70 ± 1.37	8.30 ± 0.31	> 50	NT	> 2.4
C2	9.22 ± 0.48	8.42 ± 0.30	7.73 ± 0.22	46.75 ± 2.11	NT	5.1
C3	22.04 ± 1.20	17.92 ± 1.43	23.57 ± 0.83	> 50	NT	> 2.3
5-FU	18.65 ± 1.31	6.46 ± 0.38	2.05 ± 0.11	NT	NT	NC

[a] IC_{50}: half inhibitory concentrations measured by the MTT assay. The values are expressed as averages ± standard deviations of three independent experiments.
[b] SI: selectivity index. It was calculated as: $SI = IC_{50(L\text{-}02)}/IC_{50(Bel\text{-}7402)}$.
[c] NT: not tested.
[d] NC: not calculated.

hydrogen sulfide moiety did not provide superior cytotoxicity and seem to be tipping the balance from properties of natural product toward a profile more resemble the H_2S donors, as showed in Table 1. This was supported by sole exception of **B1**, whose skeleton incorporated only one ADTOH at 14-OH with phthalic anhydride linker, for slightly improved efficacy against Bel-7402 and SGC-7901 cells. Aforementioned sizable decline in efficacy for both hybrids from parental enmein-type diterpenoid **2** was clear indication that they failed to either retain the benefits of natural products or gain synergetic effects on antitumor activity. A more intricate picture presented itself regarding the antiproliferative activities of enmein-type diterpenoid **3** based hybrids **C1–3**. First, all three conjugates exhibited better efficacy for both malignant and normal cells than enmein-type core **3**, but **C1** and **C3** disclosed no improvement of cytotoxicity over oridonin **1** in all tumor cell lines with sole exception of **C1** against A549 lung cancer cell line (IC_{50} at 8.30 μM for **C1** and 18.15 μM for **1**). The best ADTOH conjugated compound **C2**, which introduced an ADTOH moiety to 14-OH via glutaric anhydride, possessed stronger antiproliferative activities and better safety than any parental molecules. It indicated that linear linker held advantage over benzene ring. And the three carbon bridge was slightly better than two, which suggested longer carbon chain benefited the antiproliferative efficacy. Beside superior cytotoxic activities (9.22, 8.42 and 7.73 μM of IC_{50} for three tumor cells, respectively), SI were increased from 2.5 of oridonin (**1**) to 5.1. Yet **C2**'s antiproliferative activity only surpassed that of positive control, 5-FU, in Bel-7402 cells for IC_{50} of 9.22 μM over 18.65 μM. At last, the most effective one of all target hybrids, compound **A1** of enmein-type core **2** conjugated directly with α-thioctic acid displayed low IC_{50} values over all cancer cell lines (2.16 μM of Bel-7402 cells, 5.07 μM of SGC-7901 cells and 6.98 μM for A549 cells) and exerted stronger effects in Bel-7402 and SGC-7901 cells than that of 5-FU, but lagged behind in A549 cells for IC_{50} of 6.98 μM compared to 2.05 μM. In spite of higher cytotoxicity against L-02 normal liver cells, much stronger effect over Bel-7402 cells ensured an improved SI of 7.3. Further assay confirmed the safety of hybrid **A1** for similar low antiproliferative activity against human normal peripheral blood mononuclear cell line with an IC_{50} value of 14.15 μM. Evidently, compound **A1** was most suitable for in depth exploration into underlining mode of action for its antiproliferative efficacy.

2.2.2. H_2S release experiment

The ability of all target compounds to release H_2S was measured by methylene blue (MB^+) experiment according to relevant literature [83]. As displayed in Fig. 2, selected compounds experienced fast release of H_2S with half-time well under 5 min and reach peak concentration within 50 min. Additionally, a three-tier concentration of H_2S generation could be drawn from each release curve, with thioctic acid derivative (**A1**) at the top, oxidated enmein-type core **3** derivatives (**C1–3**) at the bottom and enmein-type core **2** derivatives (**B1–4**) placed at middle (All release curves and standard curve were presented in Supporting Information). Hybrid **A1** demonstrated the highest H_2S generation of all compounds tested, which in accordance with their MTT results. In contrast to the antiproliferative assay, hybrids **C1–3** were found with lowest average H_2S release of 6.87 μM and displayed moderate cytotoxicity against Bel-7402, SGC-7901 and A-549 cancer cell lines. While hybrids **B1–4** manifested higher H_2S release (with single substituted hybrid **B1** recorded slightly lower concentration than dual-esterficated structures) between 7.51 and 10.42 μM, yet they failed to show antiproliferative activities except **B1**. Whereas thioctic acid hybrid **A1** gained the synergetic effects we hoped to realize.

2.2.3. Cell cycle analysis

Persistent tumor cell proliferation relied on continual cell cycle progression [74,75], each cyclic phase was a crucial part of a proportional equilibrium. A disruption of certain phase of cell cycle could reduce cell division and suppress tumor growth. Hence, **A1**'s activity on cell cycle arrest in Bel-7402 cells was examined through flow cytometry using propidium iodide (PI) to stain chromatin for a set of analysis. As delineated in Fig. 3, the percentage of Bel-7402 cells stranded in G1 phase gave a steady rise from 31.27% of DMSO treated control to 34.13%, 43.66% and 52.62% for 1, 2 and 4 μM concentrations of **A1** added in the tests, respectively. Therefore, **A1** arrested Bel-7402 cell cycle at G1 phase.

2.2.4. The morphological analysis by Hoechst 33258 staining

Intervention of cell cycle progression could initiated the process of apoptosis, which entailed irreversible detriment of chromatic contents and dysfunctions of nuclei activities. A set of morphological transformations (cell shrinkage, chromatin condensation, disruption of cell membrane and fragmentation of cell nuclei) accompanied this damage was apt for observation of apoptosis [76]. Hence, **A1** treated Bel-7402 cells were subjected to Hoechst 33258 staining and examined by fluorescent microscope to certify apoptosis participation into **A1** induced antiproliferative activity. Testing results in Fig. 4 demonstrated that control cells without **Al** treatment presented a large overlapping cellular shape with deep blue color, while with **A1** presence (1, 2 and 4 μM), tumor cells displayed downgraded cell size shrunk to tight blue dots with scattered nuclear contents in sharp points, which clearly indicated chromatin condensation and nuclei disintegration. This results confirmed apoptosis was induced in **A1** treated Bel-7402 cells.

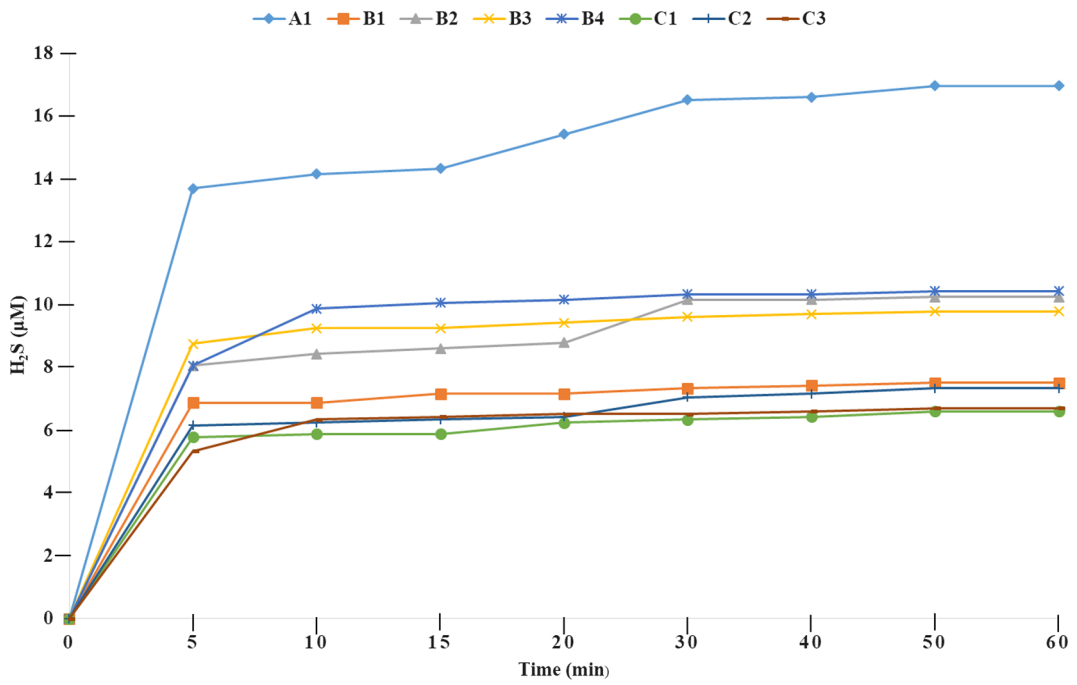

Fig. 2. H_2S-releasing ability of target compounds. The values are expressed as averages of three independent experiments.

2.2.5. Cell apoptosis assay

As a process of programmed cell death, apoptosis was triggered when normal cells exceeded life limits or suffered irreversible damage. But tumor cells could suppress apoptosis considerably to gain incessant growth [77]. Therefore, induction and elevation of apoptotic cells in tumor tissues was crucial for cancer treatment. Hence, an annexin V-FITC/PI binding assay was carried out to explore **A1** induced apoptosis in Bel-7402 cells. **A1** (1, 2 and 4 μM) was added and the proportions of cells went through apoptosis were certified by flow cytometry. Testing results were compiled in Fig. 5, which exhibited conspicuous escalation

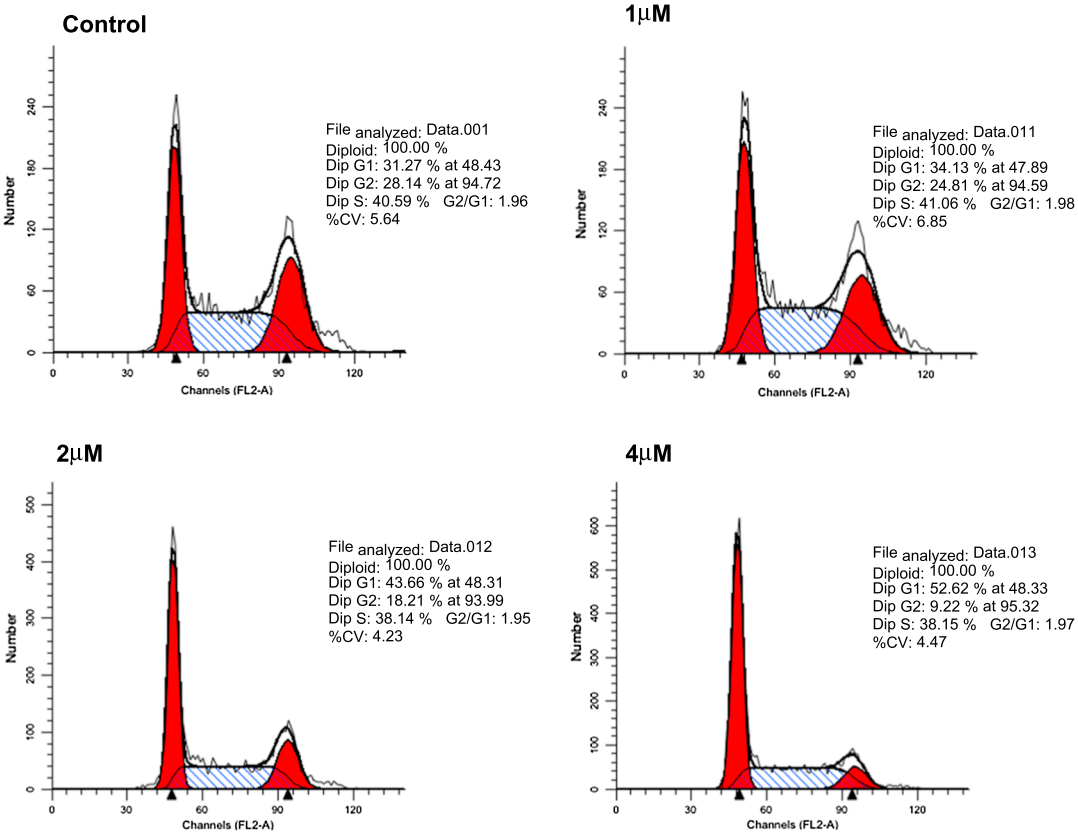

Fig. 3. Influence of the cell cycle arrest of G1 phase by **A1** in Bel-7402 cells: Bel-7402 cells were incubated with the indicated concentrations of **A1** for 24 h and the cells were stained with PI. Cellular DNA content, for cell cycle distribution analysis, was measured using a flow cytometer. The diagrams showed the distribution of the cells according to their DNA content. The inserts gave the percentages in different cell cycle phases.

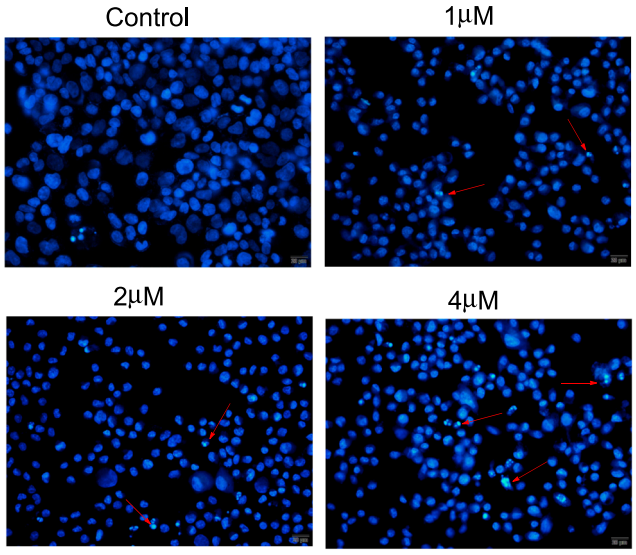

Fig. 4. Hoechst staining of **A1** treated Bel-7402 cells. Cells were treated with the indicated concentrations of **A1** or vehicle control for 48 h, stained with Hoechst 33258 and examined with a fluorescent microscope.

of apoptotic cells in **A1** treated Bel-7402 cells from 5.60% of vehicle control to 18.34% (1 μM), 31.83% (2 μM) and 61.98% (4 μM) for different concentrations applied in a dose-dependent manner. Overall, a substantial apoptotic activity was induced in **A1** treated Bel-7402 cells.

2.2.6. Mitochondria membrane potential analysis

Prominent changes of mitochondria membrane integrity were strong indication of apoptosis in cancer cell lines, which manifested itself via potential collapse throughout inner and outer layers of mitochondrial membranes. After the inner transmembrane was affected, the dissipation of its potential increased permeability of mitochondrial membrane and hence the transition between two sides, which in turn facilitated transmembrane movement of pro-apoptotic proteins [78]. Additionally, intrinsic mitochondria pathway was closely involved in H_2S derivatives induced apoptosis according to literature with the mediative role of endogenous H_2S molecules was recognized [79]. To verify **A1** induced apoptosis of Bel-7402 cells whether involved mitochondria pathway, a staining assay with flow cytometry to measure mitochondrial membrane potentials was conducted, in which target cell line was co-cultured with different concentrations of **A1** (1, 2 and 4 μM) and vehicle control with DMSO. After a period of incubation, the cells were stained with selected lipophilic cationic fluorescent mitochondrial probe, 5,5′,6,6′-tetrachloro-1,1′,3,3′-tetraethylbenzimidazol-carbocyanine iodide (JC-1). As showed in Fig. 6, the percentile of cells undergone apoptotic process risen from 0.48% of control, to 19.66%, 34.16% and 58.55% in a dose-dependent manner, for increased concentrations of **A1** added. The apoptosis **A1** induced in Bel-7402 cells involved intrinsic mitochondria pathway.

2.2.7. Effects on apoptosis-related proteins

The *dysfunction and abnormal expression of some key apoptotic proteins* was clear sign of carcinogenesis. Cancer cells avoided programmed cell death partly through obstructing the signals of pro-apoptotic proteins or other gasotransmitters then proliferated relentlessly [80]. Among them, important Bcl-2 family protein members like Bcl-2, Bcl-xL and Bax regulated intrinsic mitochondria pathway through a crucial balance between pro- and anti-apoptotic effects that mediated membrane permeabilization. The insertion of pro-apoptosis protein Bax into mitochondrial outer membrane uplifted the permeabilization and facilitated further release. But anti-apoptotic proteins Bcl-2 and Bcl-xL

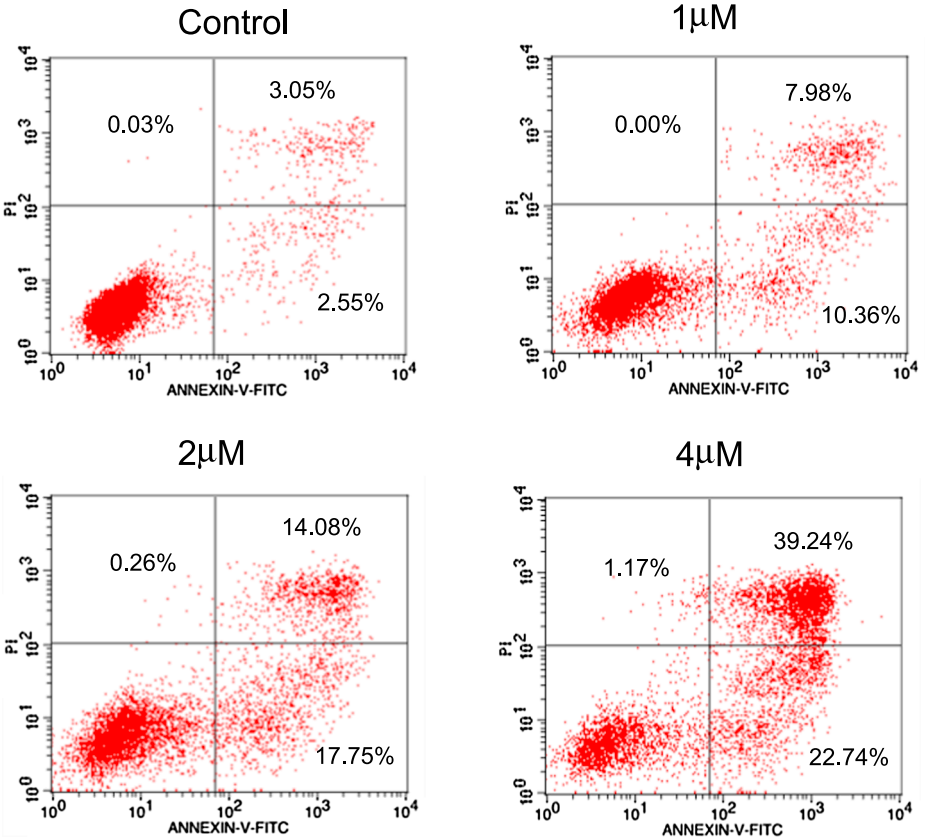

Fig. 5. Apoptosis in Bel-7402 cells by treatment with **A1**: Bel-7402 cells were incubated with different concentrations of **A1** for 24 h and the cells were stained with annexin V-FITC and PI, followed by flow cytometry analysis.

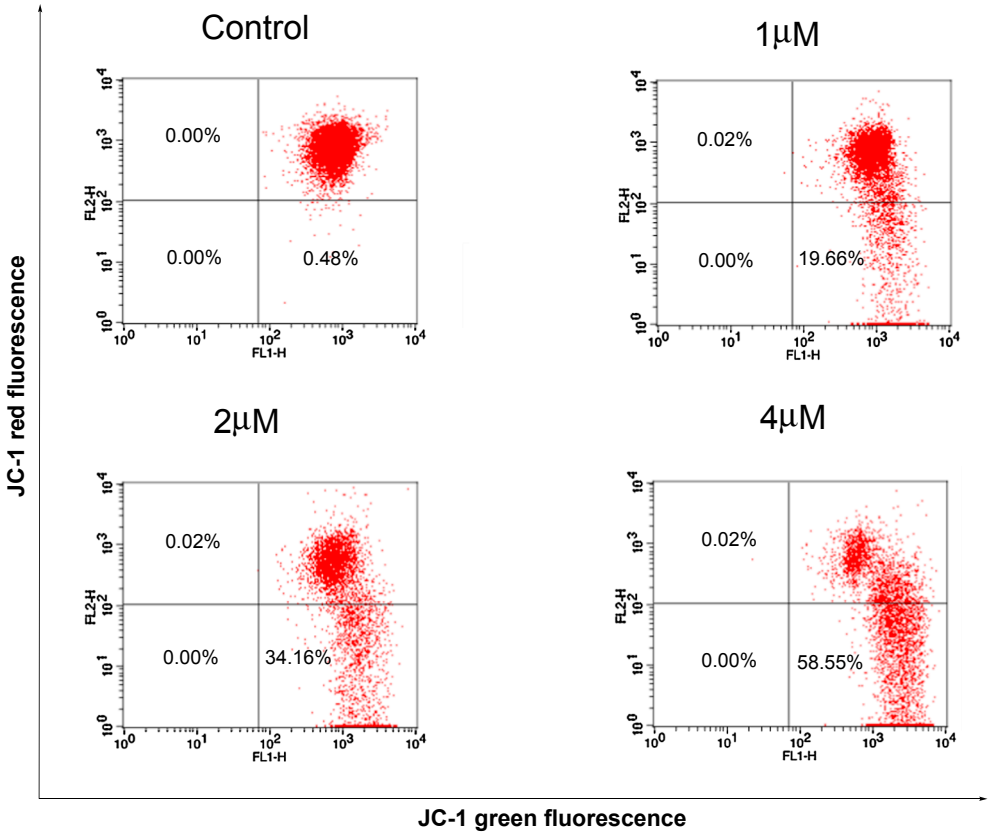

Fig. 6. Effects of **A1** on the mitochondrial membrane potentials of Bel-7402 cells: Bel-7402 cells were incubated with the indicated concentrations of **A1** for 48 h prior to staining with JC-1.

reversed the permeabilization of membrane and in turn the protein release via inhibition of Bax by direct binding. Tip the scale from overexpression of Bcl-2 and Bcl-xL in various cancers to increased levels of Bax for apoptotic induction was sound strategy for chemotherapy. Once released into outer cytoplasm, cytochrome *c* then bound to apoptotic protease activating factor-1 (Apaf-1) and (d)ATP to assemble a polyprotein complex known as apoptosome, which functioned through activation of downstream apoptotic protein caspase-9. As an indispensable factor in introducing apoptosis, caspase-9 then sought out important precursor procaspase-3 for a proteolytic cleavage of redundant part of this inactive proenzyme [81,82]. Finally, the activated caspase-3 would take up the role as executioner caspase to bring about full cellular apoptosis [83]. In order to uncover the mode of action behind the **A1** induced apoptosis in Bel-7402 cells, several selected apoptotic proteins involved in intrinsic mitochondria pathway were subjugated to Western blot assay of correspondent antibodies and their altered expression throughout apoptotic process was recorded. As Fig. 7 displayed, a notable upregulation of pro-apoptotic protein Bax, caspase-3 and cytochrome *c* were observed, in accordance to the decreased expression of zymogen procaspase-3. While anti-apoptotic proteins Bcl-2 and Bcl-xL demonstrated evident under-expression over the same time. Aforementioned results explained that a mechanism involved a set of apoptosis related proteins centered by mitochondria pathway mediated **A1** induced apoptosis in Bel-7402 cells.

3. Conclusion

Overall, we designed and synthesized a series of enmein derivatives conjugated with hydrogen sulfide donating moieties and their antiproliferative activities were evaluated in search of new drug candidates. Half of tested compounds exhibited improved efficacy over enmein-type diterpenoids and H_2S donors. All compounds demonstrated fast H_2S release with highest concentration founded in thioctic acid hybrid **A1**. **A1** also showed the most promising inhibitory effects against Bel-740, SGC-7901 and A549 cell lines with IC_{50} values of 2.16, 5.07 and 6.98 μM, respectively. Relatively low effects of IC_{50} values at 15.81 μM and 14.15 μM over human normal L-02 and PBMC cell lines were also noted. Furthermore, increased safety was also observed. The SI of **A1**, calculated between tumor and normal liver cell lines, stood at 7.3, which was highest among all tested compounds. The following biological assays uncovered central role of apoptosis in the **A1** mediated cell death event. Further exploration confirmed that G1 phase cell cycle arrest and mitochondria membrane potential collapse were involved in **A1** induced apoptosis in Bel-7402 cells. Western blot experiment demonstrated that a series of apoptotic related proteins were participated in apoptotic induction of **A1**, in which Bax, caspase-3 and cytochrome *c* went through escalation while Bcl-2, Bcl-xL and procaspase-3 levels of expression decreased notably. Hence, a hybrid **A1** was synthesized and antiproliferative evaluation certified its potential for a candidate in future anticancer therapeutics.

4. Experimental

4.1. Chemistry

Both chemicals and solvents were acquired from commercial channels. Further purification through standard methods were used when required. Oridonin was purchased from Nanjing Zelang Biology Technology Co., Ltd with HPLC purity > 98%. ^{1}H NMR and ^{13}C NMR spectra were recorded on a Bruker ARX-400 NMR spectrometer in the indicated solvents (TMS as internal standard): the values of the chemical shifts were expressed in δ values (ppm) and the coupling constants (J) in Hz. High resolution mass spectra (HR-MS) were carried out on Agilent Q-TOF B.05.01 (B5125.2).

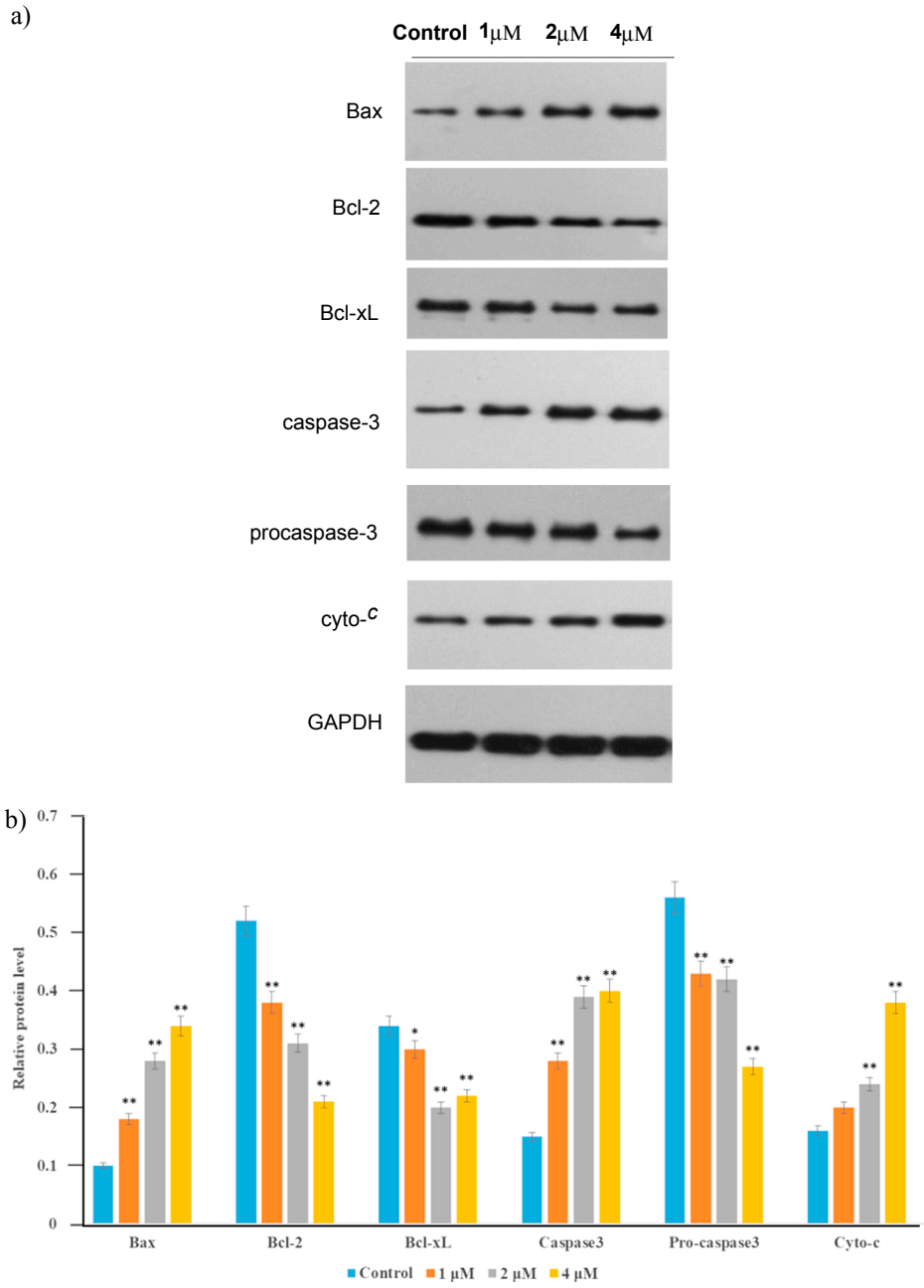

Fig. 7. (a) Western blot of apoptosis-related proteins in Bel-7402 cells after exposure to different concentrations (0, 1, 2 and 4 μM) of **A1** for 48 h. (b) Quantitative analysis showing the levels of each protein relative to control GAPDH: $^{*}p < 0.05$, $^{**}p < 0.01$ vs. vehicle control.

4.1.1. General procedures to synthesize enmein-type diterpenoids and target hybrids

Pyridine hydrochloride (0.68 mg, 5.9 mmol) was mixed with anethole trithione (0.25 mg, 1 mmol), and then heated to 215 °C till the solids melt with argon protection. After the temperature cooled to 100 °C, water (200 mL) was poured into the reaction followed by a quick filter. The crude product was then added into 10% NaOH (10 mL) and stirred for 4 h. After second filtration, the resulting precipitate was dissolved in water (50 mL), and carefully acidified to pH 2 with concentrated hydrochloric acid. The red crystal was washed to neutral by water, then dried in room temperature to afford ADTOH. Oridonin (1.08 g, 3.0 mmol) was added in 50 mL water and mixed with sodium periodate (2.57 g, 12.0 mmol) and stirred for 48 h to afford enmein-type diterpenoid **2**. The mixture was then extracted with DCM (3 × 50 mL). The combined organic layer was washed with brine, dried over anhydrous Na_2SO_4 and concentrated in vacuo. Enmein-type diterpenoid **2** (500 mg, 1.4 mmol) was dissolved in 50 mL acetone, and Jones reagent (1700 μL, 4.3 mmol) was dropped in at 0 °C to furnish enmein-type diterpenoid **3** after 30 min. Small amount of isopropanol was added dropwise to quench the mixture and then poured into 20 mL water, and extracted with DCM (3 × 20 mL). The combined organic layer was then washed with brine, dried over anhydrous Na_2SO_4 and concentrated in vacuo. Enmein-type diterpenoid **2** (36 mg, 0.1 mmol) was added into 5 mL DCM and reacted with thioctic acid (21 mg, 0.1 mmol) in presence of EDCI (134 mg, 0.7 mmol) and DMAP (0.04 mmol, 5 mg) for 12 h. Then, the mixture was poured into 10 mL 10% HCl and 10 mL water, and extracted with DCM (3 × 10 mL). The combined organic layer was washed with brine, dried over anhydrous Na_2SO_4, and concentrated in vacuo. The target compound **A1** was attained by purification with flash column chromatography (MeOH/DCM 1:100, v/v). Different enmein-type diterpenoids (108 mg, 0.3 mmol) were dissolved in 5 mL DCM and reacted with the corresponding anhydride (0.6 mmol), under the

condition of TEA (320 μL, 1.5 mmol) and DMAP (5 mg, 0.04 mmol). After 4–8 h in room temperature, the reaction was poured into 10 mL 10% HCl and 10 mL water, and extracted with DCM (3 × 10 mL). The combined organic layer was washed with brine, dried over anhydrous Na_2SO_4, and concentrated in vacuo, then used without further purification. Intermediates **6–12** (0.1 mmol) were dissolved in 5 mL DCM at −5 °C, and sequentially treated with DCC (31 mg, 0.15 mmol, added dropwise in DCM) and DMAP (5 mg, 0.04 mmol). After 8–12 h, the reactions were poured into 10 mL 10% HCl and 10 mL water and extracted with DCM (3 × 10 mL). The combined organic layers were washed with brine, dried over anhydrous Na_2SO_4, and concentrated in vacuo. The target products **B1–4** and **C1–3** were obtained through purification of flash column chromatography (MeOH/DCM 1:400, v/v).

*4.1.1.1. Compound **A1***. Yellow crystal, yield: 14%. ^{1}H NMR ($CDCl_3$, 400 M Hz), δ (ppm): 6.21 (1H, s, 17-CH_2), 5.72 (1H, s, 17-CH_2), 5.57 (1H, s, 6-CH), 5.33 (1H, s, 14-CH), 4.56 (1H, dd, J = 5.77, 11.53 Hz, 1-CH), 4.07, 3.93 (each 1H, d, J = 9.42 Hz, 20-CH_2), 2.73 (1H, dd, J = 12.97, 5.39 Hz, 8′-CH), 2.44 (1H, m, 8′-CH), 2.29 (1H, m, 6′-CH), 1.90 (2H, m, 7′-CH_2), 1.26 (4H, s, 3′,4′-CH_2), 1.02 (3H, s, 18-CH_3), 0.96 (3H, s, 19-CH_3); ^{13}C NMR ($CDCl_3$, 100 M Hz), δ (ppm): 198.03, 173.15, 166.97, 147.75, 120.31, 101.74, 76.02, 74.53, 73.72, 60.16, 56.34, 53.77, 49.88, 48.47, 40.69, 40.22, 38.46, 37.03, 34.44, 33.88, 33.79, 32.89, 31.00, 29.73, 28.57, 28.50, 23.21, 23.03, 19.77; HRMS (ESI) *m/z* calcd for $C_{28}H_{38}O_7S_2$ $[M + Na]^+$ 573.1951, found 573.1967.

*4.1.1.2. Compound **B1***. Red crystal, yield: 19%. ^{1}H NMR ($CDCl_3$, 400 M Hz), δ (ppm): 7.84 (1H, d, J = 7.40 Hz, 6′-H), 7.69 (1H, d, J = 7.44 Hz, 3′-H), 7.64 (1H, t, J = 7.40 Hz, 5′-H), 7.59 (1H, d, J = 7.40 Hz, 4′-H), 7.47, 7.73 (each 2H, d, $J_A = J_B$ = 8.68 Hz, Ar-H), 7.43 (1H, s, 8″-H), 6.36 (1H, s, 14-CH), 4.40 (1H, m, 1-CH), 4.14, 3.83 (each 1H, d, J = 9.32 Hz, 20-CH_2), 2.95 (1H, m, 13-CH), 1.08 (3H, s, 18-CH_3), 1.06 (3H, s, 19-CH_3); ^{13}C NMR ($CDCl_3$, 100 M Hz), δ (ppm): 215.54, 189.01, 175.86, 173.06, 171.62, 165.85, 165.47, 153.71, 147.65, 140.62, 136.11, 132.15, 131.90, 131.75, 130.74, 129.53, 129.27, 128.28 (×2), 128.64, 122.96 (×2), 103.47, 99.23, 75.18, 53.64, 45.59, 40.86, 37.58, 36.99, 32.74, 31.60, 23.34, 23.03, 22.20, 12.59; HRMS (ESI) *m/z* calcd for $C_{37}H_{34}O_9S_3$ $[M + H]^+$ 719.1438, found 719.1461.

*4.1.1.3. Compound **B2***. Red crystal, yield: 20%. ^{1}H NMR ($CDCl_3$, 400 M Hz), δ (ppm): 7.68 (4H, m, Ar-H), 7.40 (2H, d, J = 2.3 Hz, 8″,8‴-CH), 7.24 (4H, m, Ar-H), 6.19 (1H, d, J = 11.3 Hz, 6-CH), 5.75 (1H, s, 17-CH_2), 5.58 (1H, s, 17-CH_2), 4.56 (1H, dd, J = 11.5, 5.8 Hz, 1-CH), 4.14, 3.99 (each 1H, d, J = 9.6 Hz, 20-CH_2), 3.19 (1H, d, J = 9.5 Hz, 13-CH), 2.94, 2.80 (4H, m, 2′,2‴-H), 2.72, 2.59 (4H, m, 3′,3‴-H), 1.08 (3H, s, 18-CH_3), 1.03 (3H, s, 19-CH_3); ^{13}C NMR ($CDCl_3$, 100 M Hz), δ (ppm): 215.50 (×2), 197.46, 171.65, 171.49, 170.59, 170.34, 166.65, 153.47, 153.36, 147.36, 136.09, 136.04, 129.38, 129.24, 128.25 (×2), 128.15 (×2), 122.90 (×2), 122.79 (×2), 120.97, 102.38, 77.22, 75.73, 75.27, 74.05, 59.80, 53.36, 49.43, 47.89, 40.39, 36.92, 32.84, 31.45 (×2), 30.02, 29.17, 28.99 (×2), 28.85, 23.10, 22.95 (×2), 19.76; HRMS (ESI) *m/z* calcd for $C_{46}H_{42}O_{12}S_6$ $[M + Na]^+$ 1001.0893, found 1001.0865.

*4.1.1.4. Compound **B3***. Red crystal, yield: 21%. ^{1}H NMR ($CDCl_3$, 400 M Hz), δ (ppm): 7.69 (4H, m, Ar-H), 7.40 (2H, d, J = 1.9 Hz, 8″,8‴-CH), 7.24 (4H, m, Ar-H), 6.20 (1H, d, J = 13.8 Hz, 6-CH), 5.75 (1H, s, 17-CH_2), 5.57 (1H, s, 17-CH_2), 4.59 (1H, dd, J = 11.5, 5.8 Hz, 1-CH), 4.13, 3.98 (each 1H, d, J = 9.6 Hz, 20-CH_2), 3.17 (d, J = 9.6 Hz, 13-CH), 2.65 (4H, m, 3′,3‴-H), 2.45, 2.36 (4H, m, 2′,2‴-H), 2.01 (4H, m, 4′,4‴-H), 1.06 (3H, s, 18-CH_3), 1.03 (3H, s, 19-CH_3); ^{13}C NMR ($CDCl_3$, 100 M Hz), δ (ppm): 215.50 (×2), 197.57, 172.44, 171.53, 171.16, 170.93, 170.75, 153.55, 153.42, 147.44, 136.05, 136.01, 129.29 (×2), 129.15, 128.21 (×2), 128.17 (×2), 122.97 (×2), 122.90 (×2), 120.91, 101.65, 77.23, 75.71, 75.16, 73.75, 59.90, 53.21, 49.53, 47.95, 40.44, 36.93, 33.30, 33.00, 32.87, 32.83, 31.42, 29.95, 29.71, 23.10, 22.95, 19.86, 19.50, 19.42; HRMS (ESI) *m/z* calcd for $C_{48}H_{46}O_{12}S_6$ $[M + Na]^+$ 1029.1206, found 1029.1157.

*4.1.1.5. Compound **B4***. Red crystal, yield: 25%. ^{1}H NMR ($CDCl_3$, 400 M Hz), δ (ppm): 8.11 (1H, s, 8‴-CH), 7.92, 7.83, 7.54 (4H, m, 3″,3‴,6″,6‴-H), 7.74, 7.43 (8H, m, Ar-H), 7.62 (4H, m, 4″,4‴,5″,5‴-H), 7.39 (1H, s, 8″-CH), 6.37 (1H, s, 6-CH), 5.86 (1H, s, 17-CH_2), 5.50 (1H, s, 17-CH_2), 4.61 (1H, dd, J = 11.4, 5.8 Hz, 1-CH), 4.20 (1H, d, J = 9.7 Hz, 20-CH_2), 4.07 (1H, d, J = 9.7 Hz, 20-CH_2), 3.23 (1H, d, J = 9.3 Hz, 13-CH), 1.09 (3H, s, 18-CH_3), 1.06 (3H, s, 19-CH_3); ^{13}C NMR ($CDCl_3$, 100 M Hz), δ (ppm): 215.51 (×2), 197.39, 171.63, 171.50, 166.25, 165.15, 165.05, 153.66, 147.39, 136.12 (×2), 132.66, 132.07, 131.83, 131.69, 131.60, 131.46, 131.01, 130.02, 129.74 (×2), 129.55, 129.33, 129.24, 128.68, 128.33 (×2), 128.24 (2), 123.03 (×2), 122.80 (×2), 120.92, 103.52, 77.23, 75.79, 75.39, 74.71, 62.71, 59.66, 53.62, 49.49, 48.04, 40.25, 36.97, 32.84, 31.52, 30.01, 23.11, 22.97, 19.71; HRMS (ESI) *m/z* calcd for $C_{54}H_{42}O_{12}S_6$ $[M + Na]^+$ 1097.0893, found 1097.0839.

*4.1.1.6. Compound **C1***. Red crystal, yield: 55%. ^{1}H NMR ($CDCl_3$, 400 M Hz), δ (ppm): 7.40 (1H, s, 8″-H), 7.24, 7.67 (each 2H, d, $J_A = J_B$ = 8.64 Hz, Ar-H), 6.25 (1H, s, 14-CH), 5.73 (1H, s, 17-CH_2), 5.62 (1H, s, 17-CH_2), 4.57 (1H, m, 1-CH), 4.03, 4.34 (each 1H, d, J = 10.16 Hz, 20-CH_2), 3.20 (1H, d, J = 9.44 Hz, 13-CH), 2.83, 2.93 (2H, m, 2′-H), 2.72 (2H, m, 3′-H), 1.22 (3H, s, 18-CH_3), 1.07 (3H, s, 19-CH_3); ^{13}C NMR ($CDCl_3$, 100 M Hz), δ (ppm): 215.51, 196.91, 175.16, 171.70, 171.62, 170.25, 166.14, 153.48, 146.77, 136.04, 129.26, 128.15 (×2), 122.88 (×2), 121.77, 74.54, 73.81, 71.26, 59.44, 50.80, 47.44, 45.92, 40.20, 36.38, 33.07, 32.26, 29.69, 29.52, 28.98, 23.63, 23.07, 19.15; HRMS (ESI) *m/z* calcd for $C_{33}H_{32}O_9S_3$ $[M + H]^+$ 669.1281, found 669.1275.

*4.1.1.7. Compound **C2***. Red crystal, yield: 6%. ^{1}H NMR ($CDCl_3$, 400 M Hz), δ (ppm): 7.40 (1H, s, 8″-H), 7.22, 7.67 (each 2H, d, $J_A = J_B$ = 8.60 Hz, Ar-H), 6.27 (1H, s, 14-CH), 5.73 (1H, s, 17-CH_2), 5.64 (1H, s, 17-CH_2), 4.59 (1H, m, 1-CH), 4.03, 3.34 (each 1H, d, J = 10.16 Hz, 20-CH_2), 3.18 (1H, d, J = 9.36 Hz, 13-CH), 2.63 (2H, m, 3′-H), 2.45 (2H, t, J = 7.04 Hz, 4′-H), 2.01 (2H, t, J = 7.28 Hz, 2′-H), 1.22 (3H, s, 18-CH_3), 1.07 (3H, s, 19-CH_3); ^{13}C NMR ($CDCl_3$, 100 M Hz), δ (ppm): 215.50, 196.98, 175.22, 172.52, 171.73, 170.90, 166.20, 153.55, 146.88, 136.01, 129.16 (×2), 122.96 (×2), 121.66, 74.50, 73.53, 71.30, 59.51, 50.79, 47.43, 45.92, 40.24, 36.38, 33.07, 32.96, 32.77, 32.27, 29.53, 23.63, 23.06, 19.38, 19.17; HRMS (ESI) *m/z* calcd for $C_{34}H_{34}O_9S_3$ $[M + H]^+$ 683.1438, found 683.1452.

*4.1.1.8. Compound **C3***. Red crystal, yield: 57%. ^{1}H NMR ($CDCl_3$, 400 M Hz), δ (ppm): 7.94 (1H, m, 6′-CH), 7.81 (1H, m, 3′-CH), 7.74, 7.41 (each 2H, d, $J_A = J_B$ = 8.64 Hz, Ar-H), 7.62 (2H, m, 4′, 5′-CH), 7.43 (1H, s, 8″-CH), 6.24 (1H, s, 17-CH_2), 5.88 (1H, s, 17-CH_2), 5.58 (1H, s, 14-CH), 4.64 (1H, dd, J = 5.66, 11.50 Hz, 1-CH), 4.37, 4.07 (each 1H, d, J = 9.32 Hz, 20-CH_2), 2.63 (1H, m, 13-CH), 1.22 (3H, s, 18-CH_3), 1.07 (3H, s, 19-CH_3); ^{13}C NMR ($CDCl_3$, 100 M Hz), δ (ppm): 215.50, 197.05, 175.19, 171.51, 166.84, 165.86, 165.01, 153.65, 146.70, 136.11, 132.69, 131.66, 131.62, 129.95, 129.74, 129.53, 129.32, 128.26 (×2), 123.03 (×2), 121.83, 74.59, 74.53, 71.32, 59.39, 50.78, 47.57, 46.10, 40.17, 36.36, 33.09, 32.27, 29.53, 23.64, 23.08, 19.18; HRMS (ESI) *m/z* calcd for $C_{37}H_{32}O_9S_3$ $[M + Na]^+$ 739.1101, found 739.1132.

4.2. MTT assay

The selected cells were cultured in a standard 96-well plates and co-treated with target compounds for designated concentrations in a triplicate fashion. The incubation period settled for 72 h. The advent of MTT mixture (20 μL, 5 mg/mL) then DMSO (150 μL/well) for 10 min

was soon followed. A microplate reader (BIO-RAD Instruments Inc. 550, Hercules, CA, USA) was utilized to collect absorbance (OD) data at 490 nm wavelength. The test results were compared with that of positive control 5-FU. Antiproliferative activity examination was recorded in the form of half inhibition rate (IC_{50}), and three tumor and two normal cell lines were chosen for this assay [84].

4.3. H_2S release experiment

First, the stock solution of Na_2S (20 mM) were prepared in sodium phosphate buffer in 100 mL volumetric flask. Than aliquots of Na_2S solution were transferred to 50 mL volumetric flask to produce standard solutions of 5, 10, 20, 40, 60, 80, 100 and 150 μM, respectively. Took 1 mL of solution from each volumetric flask to react with prepared methylene blue (MB^+) cocktail which included 200 μL of 30 mM $FeCl_3$ in 1.2 M HCl, 200 μL of 20 mM *N,N*-dimethyl-1,4-phenylenediamine sulfate in 7.2 M HCl and 100 μL of 1%w/v of $Zn(OAc)_2$ in H_2O at room temperature for 20 min and repeated three times. The absorbance of each resulting mixture was recorded at 670 nm in UV–Vis spectrophotometer.

Afterwards, each hybrid was dissolved in THF solution to form a 40 mM mixture. Meanwhile, a buffer solution of 1 mM TCEP or L-cysteine was prepared in a 30 mL volumetric flask. Than both solutions were transferred to 100 mL flask for constant stir. An amount of 2000 μL was removed then added to colorimetric cuvette pre-treated with methylene blue (MB^+) cocktail for 20 min at selected time point (5, 10, 15, 20, 30, 40, 50 and 60 min). The absorbance of each test was recorded and the volume of H_2S released was obtained through standard curve [67].

4.4. Cell cycle analysis

First, 6-well plates which treated with Bel-7402 cells were cultured in a period of 24 h at 37 °C. After that compound **A1** in designated dosage prepared in DMSO joined cell culture in accordance with triplicate method. While control cell received DMSO without any target compound. Co-culture ended after 48 h and all cells were subjugated to centrifugation then fixed with 70% ethanol for the night at exact 4 °C. Another suspension was carried out in PBS mixture (include 100 μL RNase A and 400 μL PI). Finally, the indication of cell cycle, distribution of DNA content was measured by flow cytometry (FACS Calibur Becton-Dickinson, Franklin Lake, NJ, USA) [85].

4.5. Hoechst 333258 staining

Hoechst staining was chosen to examine the change in morphology of nuclei. By the same method of cell cycle assay, Bel-7402 cells were cultured in a period of 24 h at 37 °C in 6-well plates. After that compound **A1** in designated dosages was added for another 48 h incubation. Cell harvest through mild trypsinization was applied through centrifugation and two times wash with PBS. And 500 μL of Hoechst mixture (2 mg/mL) in PBS was utilized to stain the cells under the condition of room temperature, excluded light for 15 min. Finally, cells were placed in a slide after PBS wash for observation by DAPI filtered fluorescent microscope [86].

4.6. Cell apoptosis assay

At the start, Bel-7402 cells in 6-well plates were cultured in a period of 12 h. After that compound **A1** in designated dosage prepared in DMSO joined cell culture in accordance with triplicate method for 24 h. Then, cells were undergone two times PBS wash and suspension with buffer mixture for annexin V binding. The mixture was subjugated to co-culture with annexin V-FITC and then PI under the condition of 25 °C and without any light source for 15 min. This duo-staining of annxin V-FITC and PI was examined by flow cytometry for apoptosis process through the procedures provided by manufacturer [87].

4.7. Mitochondrial membrane potential assay

By the same token, Bel-7402 cells were cultured in 6-well plates. After that compound **A1** in designated dosage prepared in DMSO joined cell culture in accordance with triplicate method for 48 h. Then, cells were undergone two times PBS wash and stained with JC-1 under the condition of 25 °C and without any light source, which was strict observation of procedures provided by manufacturer (KeyGen Biotech, KGA601). Flow cytometry was employed to determine the number of cells with collapsed mitochondrial membrane potential and the data were transformed to percentage tile [88].

4.8. Western blot assay

Bel-7402 cells were treated with **A1** in designated dosage and cultured for 48 h in a triplicate fashion. Following the measurement of protein level, sodium dodecyl sulfate polyacrylamide gel electrophoresis (10% gel, SDS-PAGE) was applied to split each cell lysates, and then moved to nitrocellulose membranes. After that, tested proteins were first blocked by 5% defat milk, then thoroughly covered by monoclonal antibodies, washed with TBST, and incubated with appropriate second antibodies and followed by chemiluminescence detection. Protein visualization was achieved through Keygen ECL system (KeyGEN Biotech, Nanjing, China) while resulting images were collected by Clinx ChemiScope chemiluminescence imaging system. ChemiScope analysis program was utilized to obtain relative optical densities for individual protein [89].

Acknowledgment

This paper was financially supported by the National Natural Science Foundation of China (21772124, 21502121), Natural Science Foundation of Liaoning Province (20170540858), Project Funded by China Post Doctoral Science Foundation (2017T100186), Career Development Support Plan for Young and Middle-aged Teachers in Shenyang Pharmaceutical University, and General Scientific Research Projects of Department of Education in Liaoning Province (2017LQN05).

Disclosures of financial & competing interests

The authors have no relevant affiliations or financial involvement with any organization or entity with a financial interest in or financial conflict with the subject matter or materials discussed in the manuscript.

Appendix A. Supplementary material

Supplementary data to this article can be found online at https://doi.org/10.1016/j.bioorg.2018.10.002.

References

[1] D.J. Newman, G.M. Cragg, Natural products as sources of new drugs from 1981 to 2014, J. Nat. Prod. 79 (2016) 629–661.
[2] W.S.D. Tan, W. Liao, S. Zhou, W.S.F. Wong, Is there a future for andrographolide to be an anti-inflammatory drug? Deciphering its major mechanisms of action, Biochem. Pharmacol. 139 (2017) 71–81.
[3] S. Gupta, K.P. Mishra, L. Ganju, Broad-spectrum antiviral properties of andrographolide, Arch. Virol. 162 (2017) 611–623.
[4] V. Kishore, N.S. Yarla, A. Bishayee, S. Putta, R. Malla, N.R. Neelapu, S. Challa, S. Das, Y. Shiralgi, G. Hegde, B.L. Dhananjaya, Multi-targeting andrographolide and its natural analogs as potential therapeutic agents, Curr. Top Med. Chem. 17 (2017) 845–857.
[5] Y. Qiao, Y. Huang, F. Feng, Z.G. Chen, Efficient enzymatic synthesis and antibacterial activity of andrographolide glycoside, Process Biochem. 51 (2016) 675–680.
[6] P. Panraksa, S. Ramphan, S. Khongwichit, D.R. Smith, Activity of andrographolide against dengue virus, Antiviral Res. 139 (2017) 69–78.

[7] S.M. Nabavi, S. Habtemariam, M. Daglia, N. Braidy, M.R. Loizzo, R. Tundis, S.F. Nabavi, Neuroprotective effects of ginkgolide B against ischemic stroke: A review of current literature, Curr. Top. Med. Chem. 15 (2015) 2222–2232.

[8] H. Scholtyssek, W. Damerau, R. Wessel, I. Schimke, Antioxidative activity of ginkgolides against superoxide in an aprotic environment, Chem. Biol. Interact. 106 (1997) 183–190.

[9] T. Ikezoe, S.S. Chen, X.J. Tong, D. Heber, H. Taguchi, H.P. Koeffler, Oridonin induces growth inhibition and apoptosis of a variety of human cancer cells, Int. J. Oncol. 23 (2003) 1187–1193.

[10] M. Lenoir, O. Muntaner, E. Pedruzzi, M. Roch-Arveiller, M. Tissot, K. Drieu, A. Périanin, Ginkgolide B stimulates signaling events in neutrophils and primes defense activities, Biochem. Biophys. Res. Commun. 335 (2005) 1149–1154.

[11] E. Bernabeu, M. Cagel, E. Lagomarsino, M. Moretton, D.A. Chiappetta, Paclitaxel: What has been done and the challenges remain ahead, Int. J. Pharm. 526 (2017) 474–495.

[12] M.D. De Furia, Paclitaxel (Taxol®): A new natural product with major anticancer activity, Phytomedicine 4 (1997) 273–282.

[13] F.A. Fitzpatrick, R. Wheeler, The immunopharmacology of paclitaxel (Taxol®), docetaxel (Taxotere®), and related agents, Int. Immunopharmacol. 3 (2003) 1699–1714.

[14] L.M. Li, G.Y. Li, J.X. Pu, W.L. Xiao, L.S. Ding, H.D. Sun, *ent*-kaurane and cembrane diterpenoids from *Isodon sculponeatus* and their cytotoxicity, J. Nat. Prod. 72 (2009) 1851–1856.

[15] F. He, W.L. Xiao, J.X. Pu, Y.L. Wu, H.B. Zhang, X.N. Li, Y. Zhao, L.B. Yang, G.Q. Chen, H.D. Sun, Cytotoxic *ent*-kaurane diterpenoids from *Isodon sinuolata*, Phytochemistry 70 (2009) 1462–1466.

[16] H.Y. Jiang, W.G. Wang, M. Zhou, H.Y. Wu, R. Zhan, X.N. Li, X. Du, Y. Li, J.X. Pu, H.D. Sun, Enmein-type 6,7-*seco*-*ent*-kauranoids from *Isodon scuponeatus*, J. Nat. Prod. 76 (2013) 2113–2119.

[17] D. Li, X. Hu, T. Han, S. Xu, T. Zhou, Z. Wang, K. Cheng, Z. Li, H. Hua, W. Xiao, J. Xu, Synthesis, biological activity, and apoptotic properties of NO-donor/enmein-type *ent*-kauranoid hybrids, Int. J. Mol. Sci. 17 (2016) 747.

[18] D. Li, S. Xu, H. Cai, L. Pei, H. Zhang, L. Wang, H. Yao, X. Wu, J. Jiang, Y. Sun, J. Xu, Enmein-type diterpenoid analogs from natural kaurene-type oridonin: Synthesis and their antitumor biological evaluation, Eur. J. Med. Chem. 64 (2013) 215–221.

[19] D. Li, X. Hu, T. Han, J. Liao, W. Xiao, S. Xu, Z. Li, Z. Wang, H. Hua, J. Xu, NO-releasing enmein-type diterpenoid derivatives with selective antiproliferative activity and effects on apoptosis-related proteins, Molecules 21 (2016) 1193.

[20] L. Wang, D. Li, S. Xu, H. Cai, H. Yao, Y. Zhang, J. Jiang, J. Xu, The conversion of oridonin to spirolactone-type or enmein-type diterpenoid: Synthesis and biological evaluation of *ent*-6,7-*seco*-oridonin derivatives as novel potential anticancer agents, Eur. J. Med. Chem. 52 (2012) 242–250.

[21] J.J. Liu, R.W. Huang, D.J. Lin, X.Y. Wu, J. Peng, X.L. Pan, Q. Lin, M. Hou, M.H. Zhang, F. Chen, Antiproliferation effects of oridonin on HPB-ALL cells and its mechanisms of action, Am. J. Hematol. 81 (2006) 86–94.

[22] Y. Liu, J.H. Liu, K. Chai, S. Tashiro, S. Onodera, T. Ikejima, Inhibition of c-Met promoted apoptosis, autophagy and loss of the mitochondrial transmembrane potential in oridonin-induced A549 lung cancer cells, J. Pharm. Pharmacol. 65 (2013) 1622–1642.

[23] S.Y. Gao, J. Li, X.Y. Qu, N. Zhu, Y.B. Ji, Downregulation of Cdk1 and cyclinB1 expression contributes to oridonin-induced cell cycle arrest at G2/M phase and growth inhibition in SGC-7901 gastric cancer cells, Asian Pac. J. Cancer Prev. 15 (2014) 6437–6441.

[24] R.Y. Chen, B. Xu, S.F. Chen, S.S. Chen, T. Zhang, J. Ren, J. Xu, Effect of oridonin-mediated hallmark changes on inflammatory pathways in human pancreatic cancer (BxPC-3) cells, World J. Gastroenterol. 20 (2014) 14895–14903.

[25] Z. Ji, Q. Tang, J. Zhang, Y. Yang, Y. Liu, Y. Pan, Oridonin-induced apoptosis in SW620 human colorectal adenocarcinoma cells, Oncol. Lett. 2 (2011) 1303–1307.

[26] H. Wang, Y. Ye, Z.L. Yu, Proteomic and functional analyses demonstrate the involvement of oxidative stress in the anticancer activities of oridonin in HepG2 cells, Oncol. Rep. 31 (2014) 2165–2172.

[27] J.B. Liu, J.Y. Yue, Preliminary study on the mechanism of oridonin-induced apoptosis in human squamous cell oesophageal carcinoma cell line EC9706, J. Int. Med. Res. 42 (2014) 984–992.

[28] L.M. Li, G.Y. Li, L.S. Ding, C. Lei, L.B. Yang, Y. Zhao, Z.Y. Weng, S.H. Li, S.X. Huang, W.L. Xiao, Q.B. Han, H.D. Sun, Sculponins A-C, three new 6,7-*seco*-*ent*-kauranoids from *Isodon sculponeatus*, Tetrahedron Lett. 48 (2007) 9100–9103.

[29] B. Jiang, A.J. Hou, M.L. Li, S.H. Li, Q.B. Han, S.J. Wang, Z.W. Lin, H.D. Sun, Cytotoxic *ent*-kaurane diterpenoids from *Isodon sculponeata*, Planta Med. 68 (2002) 921–925.

[30] H. Shi, S. He, L. He, Y.J. Pan, New diterpenoid compound from *Rabdosia macrocalyx*, Chem. J. Chin. Univ. 28 (2007) 100–102.

[31] J.X. Zhang, Z.A. He, Z.Y. Chen, Y.X. Wang, S.P. Bai, H.D. Sun, Cytotoxic *ent*-kaurane diterpenoids from *Isodon macrophyllus*, J. Asian Nat. Prod. Res. 11 (2009) 693–697.

[32] S. Xu, L. Pei, D. Li, H. Yao, H. Cai, H. Yao, X. Wu, J. Xu, Synthesis and anti-mycobacterial evaluation of natural oridonin and its enmein-type derivatives, Fitoterapia 99 (2014) 300–306.

[33] C.H. Leung, S.P. Grill, W. Lam, Q.B. Han, H.D. Sun, Y.C. Cheng, Novel mechanism of inhibition of nuclear factor-κB DNA-binding activity by diterpenoids isolated from *Isodon rubescens*, Mol. Pharmacol. 68 (2005) 286–297.

[34] T.C. Hsieh, E.K. Wijeratne, J.Y. Liang, A.L. Gunatilaka, J.M. Wu, Differential control of growth, cell cycle progression, and expression of NF-κB in human breast cancer cells MCF-7, MCF-10A, and MDA-MB-231 by ponicidin and oridonin, diterpenoids from the Chinese herb *Rabdosia rubescens*, Biochem. Biophys. Res. Commun. 337 (2005) 224–231.

[35] C.Y. Li, E.Q. Wang, Y. Cheng, J.K. Bao, Oridonin: An active diterpenoid targeting cell cycle arrest, apoptotic and autophagic pathways for cancer therapeutics, Int. J. Biochem. Cell Biol. 43 (2011) 701–704.

[36] Z. Liu, L. Ouyang, H. Peng, W.Z. Zhang, Oridonin: targeting programmed cell death pathways as an anti-tumour agent, Cell Prolif. 45 (2012) 499–507.

[37] Z. Zhao, Y. Chen, Oridonin, a promising antitumor natural product in the chemotherapy of hematological malignancies, Curr. Pharm. Biotechnol. 15 (2014) 1083–1092.

[38] S. Pavel, L. Timofey, O. Natalia, M. Alexey, P. Nadezhda, D. Sergey, B. Anton, S. Carol, K. Olga, P. Vladimir, Synergistic suppression of t(8;21)-positive leukemia cell growth by combining oridonin and MAPK1/ERK2 inhibitors, Oncotarget 8 (2017) 56991–57002.

[39] X. Gao, J. Li, M. Wang, S. Xu, W. Liu, L. Zang, Z. Li, H. Hua, J. Xu, D. Li, Novel enmein-type diterpenoid hybrids coupled with nitrogen mustards: synthesis of promising candidates for anticancer therapeutics, Eur. J. Med. Chem. 146 (2018) 588–598.

[40] E. Culotta, D.E. Koshland Jr., NO news is good news, Science 18 (1992) 1862–1865.

[41] L. Xiao, J.H. Dong, X. Teng, S. Jin, H.M. Xue, S.Y. Liu, Q. Guo, W. Shen, X.C. Ni, Y.M. Wu, Hydrogen sulfide improves endothelial dysfunction in hypertension by activating peroxisome proliferator-activated receptor delta/endothelial nitric oxide synthase signaling, J. Hypertens. 36 (2018) 651–665.

[42] Y.Y. Mok, M.S. Atan, C.Y. Ping, W.Z. Jing, M. Bhatia, S. Moochhala, P.K. Moore, Role of hydrogen sulphide in haemorrhagic shock in the rat: protective effect of inhibitors of hydrogen sulphide biosynthesis, Br. J. Pharmacol. 143 (2004) 881–889.

[43] D. Wu, J. Wang, H. Li, M. Xue, A. Ji, Y. Li, Role of hydrogen sulfide in ischemia-reperfusion injury, Oxid. Med. Cell Longev. 2015 (2015) 186908.

[44] S. Mani, A. Untereiner, L. Wu, R. Wang, Hydrogen sulfide and the pathogenesis of atherosclerosis, Antioxid. Redox Signal. 20 (2014) 805–817.

[45] R.N. Carter, N.M. Morton, Cysteine and hydrogen sulphide in the regulation of metabolism: insights from genetics and pharmacology, J. Pathol. 238 (2016) 321–332.

[46] N. Sen, Functional and molecular insights of hydrogen sulfide signaling and protein sulfhydration, J. Mol. Biol. 429 (2017) 543–561.

[47] C. Szabó, Hydrogen sulphide and its therapeutic potential, Nat. Rev. Drug Discov. 6 (2007) 917–935.

[48] M. Whiteman, S. Le Trionnaire, M. Chopra, B. Fox, J. Whatmore, Emerging role of hydrogen sulfide in health and disease: critical appraisal of biomarkers and pharmacological tools, Clin. Sci. 121 (2011) 459–488.

[49] D. Wu, M. Li, W. Tian, S. Wang, L. Cui, H. Li, H. Wang, A. Ji, Y. Li, Hydrogen sulfide acts as a double-edged sword in human hepatocellular carcinoma cells through EGFR/ERK/MMP-2 and PTEN/AKT signaling pathways, Sci. Rep. 7 (2017) 5134.

[50] S.S. Wang, Y.H. Chen, N. Chen, L.J. Wang, D.X. Chen, H.L. Weng, S. Dooley, H.G. Ding, Hydrogen sulfide promotes autophagy of hepatocellular carcinoma cells through the PI3K/Akt/mTOR signaling pathway, Cell Death Dis. 8 (2017) e2688.

[51] H. Kimura, Hydrogen sulfide: its production, release and functions, Amino Acids 41 (2011) 113–121.

[52] J.L. Wallace, J.G. Ferraz, M.N. Muscara, Hydrogen sulfide: an endogenous mediator of resolution of inflammation and injury, Antioxid. Redox Signal. 17 (2012) 58–67.

[53] H. Guo, J.W. Gai, Y. Wang, H.F. Jin, J.B. Du, J. Jin, Characterization of hydrogen sulfide and its synthases, cystathionine β–synthase and cystathionine γ–lyase, in human prostatic tissue and cells, Urology 79 (2012) 483.e1–483.e5.

[54] C. Szabo, C. Coletta, C. Chao, K. Módis, B. Szczesny, A. Papapetropoulos, M.R. Hellmich, Tumor–derived hydrogen sulfide, produced by cystathionine–β–synthase, stimulates bioenergetics, cell proliferation, and angiogenesis in colon cancer, Proc. Natl. Acad. Sci. USA 110 (2013) 12474–12479.

[55] S. Sen, B. Kawahara, D. Gupta, R. Tsai, M. Khachatryan, S. Roy-Chowdhuri, S. Bose, A. Yoon, K. Faull, R. Farias-Eisner, G. Chaudhuri, Role of cystathionine β–synthase in human breast cancer, Free Radic. Biol. Med. 86 (2015) 228–238.

[56] S. Bhattacharyya, S. Saha, K. Giri, I.R. Lanza, K.S. Nair, N.B. Jennings, C. Rodriguez-Aguayo, G. Lopez-Berestein, E. Basal, A.L. Weaver, D.W. Visscher, W. Cliby, A.K. Sood, R. Bhattacharya, P. Mukherjee, Cystathionine beta–synthase (CBS) contributes to advanced ovarian cancer progression and drug resistance, Plos One 8 (2013) e79167.

[57] M.R. Hellmich, C. Coletta, C. Chao, C. Szabo, The therapeutic potential of cystathionine β–synthetase/hydrogen sulfide inhibition in cancer, Antioxid. Redox Signal. 22 (2015) 424–448.

[58] Y. Han, F. Zeng, G. Tan, C. Yang, H. Tang, Y. Luo, J. Feng, H. Xiong, Q. Guo, Hydrogen sulfide inhibits abnormal proliferation of lymphocytes via AKT/GSK3β signal pathway in systemic lupus erythematosus patients, Cell. Physiol. Biochem. 31 (2013) 795–804.

[59] Z.W. Lee, X.Y. Teo, E.Y. Tay, C.H. Tan, T. Hagen, P.K. Moore, L.W. Deng, Utilizing hydrogen sulfide as a novel anti–cancer agent by targeting cancer glycolysis and pH imbalance, Br. J. Pharmacol. 171 (2014) 4322–4336.

[60] Z.W. Lee, J. Zhou, C.S. Chen, Y. Zhao, C.H. Tan, L. Li, P.K. Moore, L.W. Deng, The slow–releasing hydrogen sulfide donor, GYY4137, exhibits novel anti–cancer effects *in vitro* and *in vivo*, Plos One 6 (2011) e21077.

[61] K. Chegaev, B. Rolando, D. Cortese, E. Gazzano, I. Buondonno, L. Lazzarato, M. Fanelli, C.M. Hattinger, M. Serra, C. Riganti, R. Fruttero, D. Ghigo, A. Gasco, H_2S-donating doxorubicins may overcome cardiotoxicity and multidrug resistance, J. Med. Chem. 59 (2016) 4881–4889.

[62] W. Feng, X.Y. Teo, W. Novera, P.M. Ramanujulu, D. Liang, D. Huang, P.K. Moore, L.W. Deng, B.W. Dymock, Discovery of new H_2S releasing phosphordithioates and 2,3-dihydro-2-phenyl-2-sulfanylenebenzo[d][1,3,2] oxazaphospholes with improved antiproliferative activity, J. Med. Chem. 58 (2015) 6456–6480.

[63] C.T. Yang, L. Chen, S. Xu, J.J. Day, X. Li, M. Xian, Recent development of hydrogen sulfide releasing/stimulating reagents and their potential applications in cancer and

glycometabolic disorders, Front. Pharmacol. 8 (2017) 664.
[64] P.D. Cicco, E. Panza, G. Ercolano, C. Armogida, G. Sessa, G. Pirozzi, G. Cirino, J.L. Wallace, A. Ianaro, ATB-346, a novel hydrogen sulfide-releasing anti-inflammatory drug, induces apoptosis of human melanoma cells and inhibits melanoma development in vivo, Pharmacol. Res. 114 (2016) 67–73.
[65] A. Ianaro, G. Cirino, J.L. Wallace, Hydrogen sulfide-releasing anti-inflammatory drugs for chemoprevention and treatment of cancer, Pharmacol. Res. 111 (2016) 652–658.
[66] U. Hasegawa, N. Tateishi, H. Uyama, A.J. van der Vlies, Hydrolysis-sensitive dithiolethione prodrug micelles, Macromol. Biosci. 15 (2015) 1512–1522.
[67] M. Li, J. Li, T. Zhang, Q. Zhao, J. Cheng, B. Liu, Z. Wang, L. Zhao, C. Wang, Syntheses, toxicities and anti-inflammation of H_2S-donors based on nonsteroidal anti-inflammatory drugs, Eur. J. Med. Chem. 138 (2017) 51–65.
[68] Y. Zhao, H. Wang, M. Xian, Cysteine-activated hydrogen sulfide (H_2S) donors, J. Am. Chem. Soc. 133 (2011) 15–17.
[69] E. Barresi, G. Nesi, V. Citi, E. Piragine, I. Piano, S. Taliani, F. Da Settimo, S. Rapposelli, L. Testai, M.C. Breschi, C. Gargini, V. Calderone, A. Martelli, Iminothioethers as hydrogen sulfide donors: from the gasotransmitter release to the vascular effects, J. Med. Chem. 60 (2017) 7512–7523.
[70] J. Kang, A.J. Ferrell, W. Chen, D. Wang, M. Xian, Cyclic acyl disulfides and acyl selenylsulfides as the precursors for persulfides (RSSH), selenylsulfides (RSeSH), and hydrogen sulfide (H_2S), Org. Lett. 20 (2018) 852–855.
[71] M.M. Cerda, M.D. Hammers, M.S. Earp, L.N. Zakharov, M.D. Pluth, Applications of synthetic organic tetrasulfides as H_2S donors, Org. Lett. 19 (2017) 2314–2317.
[72] M. Fragai, G. Comito, L.D.C. Mannelli, R. Gualdani, V. Calderone, Lipoyl-homotaurine derivative (ADM_12) reverts oxaliplatin-induced neuropathy and reduces cancer cells malignancy by inhibiting carbonic anhydrase IX (CAIX), J. Med. Chem. 60 (2017) 9003–9011.
[73] M.R. Hellmich, C. Szabo, Hydrogen sulfide and cancer, Handb. Exp. Pharmacol. 230 (2015) 233–241.
[74] J.A. Pietenpol, Z.A. Stewart, Cell cycle checkpoint signaling: cell cycle arrest versus apoptosis, Toxicology 181 (2002) 475–481.
[75] Y. Fuchs, H. Steller, Programmed cell death in animal development and disease, Cell 147 (2011) 742–758.
[76] B. Pucci, M. Kasten, A. Giordano, Cell cycle and apoptosis, Neoplasia 4 (2000) 291–299.
[77] S. Kasibhatla, B. Tseng, Why target apoptosis in cancer treatment? Mol. Cancer Ther. 2 (2003) 573–580.
[78] M. Loeffler, G. Kroemer, The mitochondrion in cell death control: certainties and incognita, Exp. Cell Res. 256 (2000) 19–26.
[79] S. Ma, D. Zhong, P. Ma, G. Li, W. Hua, Y. Sun, N. Liu, L. Zhang, W. Zhang, Exogenous hydrogen sulfde ameliorates diabetes-associated cognitive decline by regulating the mitochondria-mediated apoptotic pathway and IL-23/IL-17 expression in db/db mice, Cell Physiol. Biochem. 41 (2017) 1838–1850.
[80] K.S. Putt, G.W. Chen, J.M. Pearson, J.S. Sandhorst, M.S. Hoagland, J.T. Kwon, S.K. Hwang, H. Jin, M.I. Churchwell, M.H. Cho, D.R. Doerge, W.G. Helferich, P.J. Hergenrother, Small-molecule activation of procaspase-3 to caspase-3 as a personalized anticancer strategy, Nat. Chem. Biol. 2 (2016) 543–550.
[81] P. Li, D. Nijhawan, I. Budihardjo, S.M. Srinivasula, M. Ahmad, E.S. Alnemri, X. Wang, Cytochrome c and dATP-dependent formation of Apaf-1/caspase-9 complex initiates an apoptotic protease cascade, Cell 91 (1997) 479–489.
[82] S.M. Srinivasula, M. Ahmad, T. Fernandes-Alnemri, E.S. Alnemri, Autoactivation of procaspase-9 by Apaf-1-mediated oligomerization, Mol. Cell 1 (1998) 949–957.
[83] S. Xu, H. Yao, S. Luo, Y.K. Zhang, D.H. Yang, D. Li, G. Wang, M. Hu, Y. Qiu, X. Wu, H. Yao, W. Xie, Z.S. Chen, J. Xu, A novel potent anticancer compound optimized from a natural oridonin scaffold induces apoptosis and cell cycle arrest through the mitochondrial pathway, J. Med. Chem. 60 (2017) 1449–1468.
[84] J. Chen, T. Wang, S. Xu, P. Zhang, A. Lin, L. Wu, H. Yao, W. Xie, Z. Zhu, J. Xu, Discovery of novel antitumor nitric oxide-donating β-elemene hybrids through inhibiting the PI3K/Akt pathway, Eur. J. Med. Chem. 135 (2017) 414–423.
[85] Z. Wen, Y. Zhang, X. Wang, X. Zeng, Z. Hu, Y. Liu, Y. Xie, G. Liang, J. Zhu, H. Luo, B. Xu, Novel 3′,5′-diprenylated chalcones inhibited the proliferation of cancer cells in vitro by inducing cell apoptosis and arresting cell cycle phase, Eur. J. Med. Chem. 133 (2017) 227–239.
[86] T. Han, J. Li, J. Xue, H. Li, F. Xu, K. Cheng, D. Li, Z. Li, M. Gao, H. Hua, Scutellarin derivatives as apoptosis inducers: Design, synthesis and biological evaluation, Eur. J. Med. Chem. 135 (2017) 270–281.
[87] K. Tian, F. Xu, X. Gao, T. Han, J. Li, H. Pan, L. Zang, D. Li, Z. Li, T. Uchita, M. Gao, H. Hua, Nitric oxide-releasing derivatives of brefeldin A as potent and highly selective anticancer agents, Eur. J. Med. Chem. 136 (2017) 131–143.
[88] J. Chen, T. Wang, S. Xu, A. Lin, H. Yao, W. Xie, Z. Zhu, J. Xu, Design, synthesis and biological evaluation of novel nitric oxide-donating protoberberine derivatives as antitumor agents, Eur. J. Med. Chem. 132 (2017) 173–183.
[89] S. Xu, H. Yao, L. Pei, M. Hu, D. Li, Y. Qiu, G. Wang, L. Wu, H. Yao, Z. Zhu, J. Xu, Design, synthesis, and biological evaluation of NAD(P)H: Quinone oxidoreductase (NQO1)-targeted oridonin prodrugs possessing indolequinone moiety for hypoxia-selective activation, Eur. J. Med. Chem. 132 (2017) 310–321.